

Spontaneous hot flow anomalies at quasi-parallel shocks:

2. Hybrid simulations

N. Omidi,¹ H. Zhang,² D. Sibeck,³ and D. Turner⁴

Received 5 July 2012; revised 2 October 2012; accepted 11 November 2012; published 31 January 2013.

[1] Motivated by recent THEMIS observations, this paper uses 2.5-D electromagnetic hybrid simulations to investigate the formation of Spontaneous Hot Flow Anomalies (SHFAs) upstream of quasi-parallel bow shocks during steady solar wind conditions and in the absence of discontinuities. The results show the formation of a large number of structures along and upstream of the quasi-parallel bow shock. Their outer edges exhibit density and magnetic field enhancements, while their cores exhibit drops in density, magnetic field, solar wind velocity, and enhancements in ion temperature. Using virtual spacecraft in the simulation, we show that the signatures of these structures in the time series data are very similar to those of SHFAs seen in THEMIS data and conclude that they correspond to SHFAs. Examination of the simulation data shows that SHFAs form as the result of foreshock cavitons interacting with the bow shock. Foreshock cavitons in turn form due to the nonlinear evolution of ULF waves generated by the interaction of the solar wind with the backstreaming ions. Because foreshock cavitons are an inherent part of the shock dissipation process, the formation of SHFAs is also an inherent part of the dissipation process leading to a highly nonuniform plasma in the quasi-parallel magnetosheath including large-scale density and magnetic field cavities.

Citation: Omidi, N., H. Zhang, D. Sibeck, and D. Turner (2013), Spontaneous hot flow anomalies at quasi-parallel shocks: 2. Hybrid simulations, *J. Geophys. Res. Space Physics*, 118, 173–180, doi: 10.1029/2012JA018099.

1. Introduction

[2] Collisionless dissipation processes at the bow shock result in reflection and/or leakage of ions into the upstream region forming the ion foreshock region [Asbridge *et al.*, 1968; Greenstadt *et al.*, 1968, 1980; Gosling *et al.*, 1978; Paschmann *et al.*, 1979; Bonifazi *et al.*, 1980a, 1980b]. The ion foreshock is populated with a variety of ULF waves [e.g. Russell and Hoppe, 1983; Le and Russell, 1992; Greenstadt *et al.*, 1995] with wave vectors toward the Sun but carried back by the solar wind in the opposite direction. Both observations and theoretical studies have also established the turbulent nature of the quasi-parallel shocks and the cyclic reformation of the shock front [e.g. Greenstadt *et al.*, 1977, 1993; Russell, 1988, Thomsen *et al.*, 1988, Thomsen *et al.*, 1990a, 1990b; Burgess, 1989; Thomas *et al.*, 1990; Winske *et al.*, 1990; Omidi *et al.*, 1990; Scholer *et al.*, 1993]. This behavior is thought to be caused by the convection of upstream generated ULF waves into the shock.

[3] In an accompanying paper, Zhang *et al.* (Zhang, H., *et al.*, Spontaneous hot flow anomalies at quasi-parallel shocks: 1. Observations, submitted to *Journal of Geophysical Research*, 2012) used THEMIS multispacecraft measurements to identify a new structure at the quasi-parallel bow shock named spontaneous hot flow anomaly (SHFA). SHFAs and hot flow anomalies (HFAs) exhibit similar signatures in spacecraft time series data that consist of enhancements in density and magnetic field in the outer part and depletions in these parameters in the core, which is also associated with increased temperature and deflected solar wind flow. However, while HFAs form due to the interaction of solar wind discontinuities with the bow shock [e.g. Schwartz *et al.*, 1988, 2000; Schwartz, 1995; Thomsen *et al.*, 1986, 1988, 1993; Paschmann *et al.*, 1988; Thomas *et al.*, 1991; Sibeck *et al.*, 1998, 1999, 2000; Lin, 1997, 2002; Lucek *et al.*, 2004; Omidi and Sibeck, 2007; Facsko *et al.*, 2008; Eastwood *et al.*, 2008; Jacobsen *et al.*, 2009], SHFAs form in the absence of discontinuities. In the past, local and global hybrid (kinetic ions, fluid electrons) simulations have been used successfully to examine the formation and impacts of HFAs at the bow shock [e.g. Thomas *et al.*, 1991; Lin, 1997, 2002; Omidi and Sibeck, 2007]. Motivated by SHFA observations, we have conducted an investigation of the quasi-parallel bow shock using global hybrid simulations. As we demonstrate here, simulations show the formation of copious structures at the quasi-parallel bow shock and foreshock whose time series signatures resemble those of SHFAs presented by Zhang *et al.* (Zhang, H., *et al.*, Spontaneous hot flow anomalies at quasi-parallel shocks: 1. Observations, submitted to

¹Solana Scientific Inc, Solana Beach, California, USA.

²University of Alaska, Fairbanks, Alaska, USA.

³NASA/GSFC, Greenbelt, Maryland, USA.

⁴IGPP/UCLA, Los Angeles, California, USA.

Corresponding author: N. Omidi, Solana Scientific Inc., Solana Beach, California, USA. (omidid@solanasci.com)

©2012. American Geophysical Union. All Rights Reserved.
2169-9380/13/2012JA018099

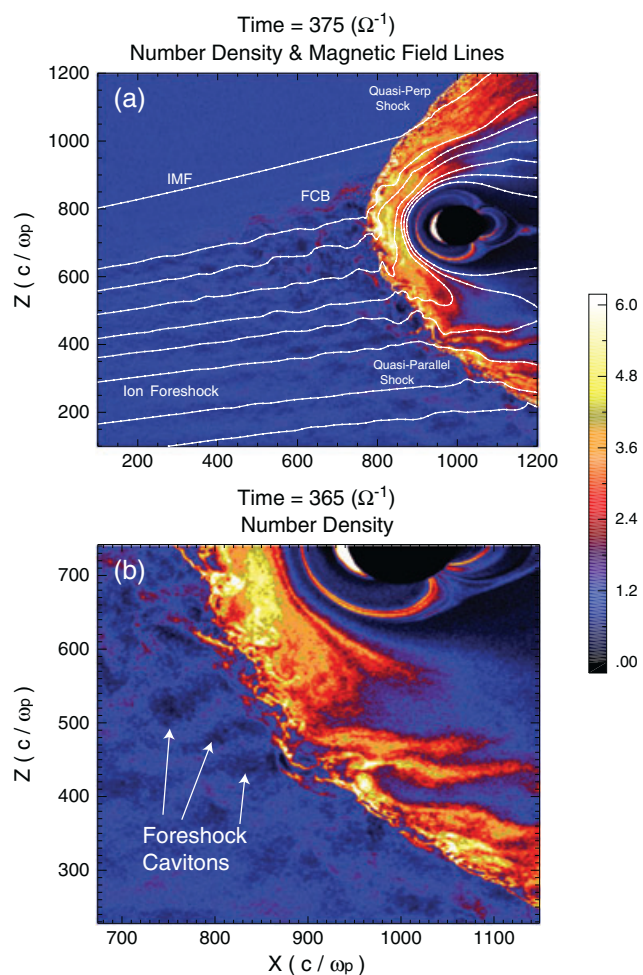


Figure 1. (a) Plasma density normalized to solar wind value and various parts of the bow shock and the ion foreshock. (b) Zoomed view of the foreshock and bow shock showing foreshock cavitons.

Journal of Geophysical Research, 2012). The results indicate that SHFAs are an inherent part of the supercritical quasi-parallel shock dissipation processes and result in highly turbulent and nonuniform magnetosheath plasma.

[4] The structure of the paper is as follows. Section 2 describes the hybrid model used in this study while the simulation results are described in section 3. Section 4 provides a summary and conclusions.

2. Hybrid Simulation Model

[5] The main tool of investigation in this study is a 2.5-D (2-D in space and 3-D in currents and electromagnetic fields) global hybrid simulation model used extensively in the past [e.g., *Omidi et al.*, 2004, 2005, 2006, 2009a, 2009b, 2010; *Omidi and Sibeck*, 2007; *Blanco-Cano et al.*, 2006a, 2006b, 2009, 2011; *Sibeck et al.*, 2008]. In electromagnetic hybrid codes, ions are treated as macroparticles and consist of one or more species (e.g., differing mass, charge, etc.), whereas electrons are treated as a massless, charge neutralizing fluid [see, e.g., *Winske and Omidi*, 1993, 1996].

[6] The model consists of a dipole inside a sphere whose surface represents the ionospheric boundary. A solar wind

type plasma with electron and ion betas (ratio of thermal to magnetic pressure) of 0.3 each and flow speed of $12 V_A$ (Alfvén speed) is uniformly loaded in the system except for the region inside the ionospheric boundary. This plasma is continuously injected from the left hand boundary throughout the whole run. The remaining boundaries remain open for the plasma to leave. Similarly, open boundary conditions are applied for the electromagnetic fields so that excited waves and turbulence in the system leave through these boundaries. The simulation box lies in the X - Z (noon-midnight meridian) plane with X along the solar wind flow direction (Sun-Earth line) and the magnetic dipole moment in the Z direction so that X corresponds to $-X_{\text{GSM}}$ and Z corresponds to Z_{GSM} . The simulation box extends 1500 ion skin depths c/ω_p (where c is the speed of light and ω_p is the ion plasma frequency) in the X and Z directions with cell size of 1 ion skin depth. The interplanetary magnetic field (IMF) lies in the X - Z plane and makes a cone angle of 10° with the X axis. To optimize the computational resources, the simulated magnetosphere is smaller (by a factor of ~ 5) than the Earth's magnetosphere. On the other hand, the simulated plasma parameters and characteristic time and spatial scales such as gyroperiod, or ion skin depth are the same as in the solar wind and magnetosphere. This ensures that the simulations are capable of generating plasma and field values and characteristic scales that can be directly compared to observations at the Earth's bow shock. As demonstrated in our earlier studies, the physical processes occurring in smaller bow shocks and magnetospheres are similar to those at the Earth's magnetosphere and much can be learned from these simulations including scaling properties of various magnetospheric processes [e.g., *Omidi et al.*, 2004, 2005, 2006, 2009a, 2009b, 2010; *Omidi and Sibeck*, 2007; *Blanco-Cano et al.*, 2006a, 2006b, 2009, 2011; *Sibeck et al.*, 2008].

3. Formation of SHFAs

[7] Figure 1a shows the plasma density (normalized to solar wind value) and magnetic field lines in a portion of the simulation domain. The quasi-perpendicular and parallel portions of the bow shock are labeled in this figure with the latter falling primarily in the Southern Hemisphere. Also labeled is the ion foreshock, upstream of the quasi-parallel shock, and the foreshock compressional boundary (FCB) that separates a highly disturbed and turbulent ion foreshock plasma from a nearly pristine like solar wind that falls inside the ion foreshock (beam) boundary [see *Sibeck et al.*, 2008; *Omidi et al.*, 2009b]. Figure 1b shows the density zoomed around the quasi-parallel shock and the ion foreshock. The latter includes regions of low density labeled foreshock cavitons. The presence of these structures was predicted by global hybrid simulations [*Lin*, 2003; *Lin and Wang*, 2005; *Omidi*, 2007] and confirmed in the ion foreshock [*Blanco-Cano et al.*, 2009, 2011; *Kajdič et al.*, 2010, 2011]. Foreshock cavitons are about an R_E (Earth radii) in size and are associated with drops in density and magnetic field in their core by as much as 50% or more and plasma and magnetic field enhancements in their outer edge. They form as a result of the nonlinear evolution of ULF waves and are carried back by the solar wind toward the bow shock. As we show here, the interaction between foreshock cavitons and the bow shock is highly significant and an inherent part of the quasi-parallel shock dissipation processes.

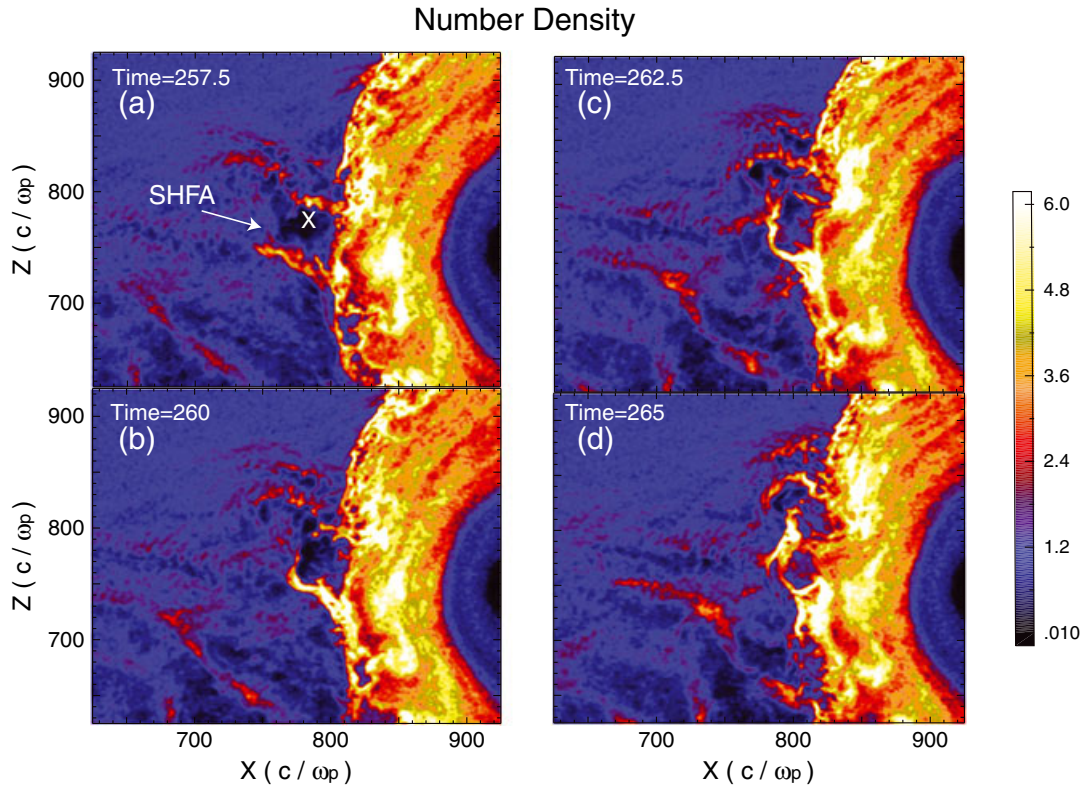


Figure 2. Plasma density normalized to solar wind value at four times (proton gyroperiods Ω^{-1}) demonstrating the interaction of SHFA with the bow shock.

[8] Although at any given time the structure of the quasi-parallel bow shock is highly turbulent, a closer examination reveals processes that occur at and upstream of the shock on a regular basis. An example of this is illustrated in Figures 2

and 3 that show the density and ion temperature (normalized to solar wind value), respectively, at four different times (normalized to proton gyroperiod Ω^{-1}) zoomed around the quasi-parallel bow shock. Ion temperature is obtained by

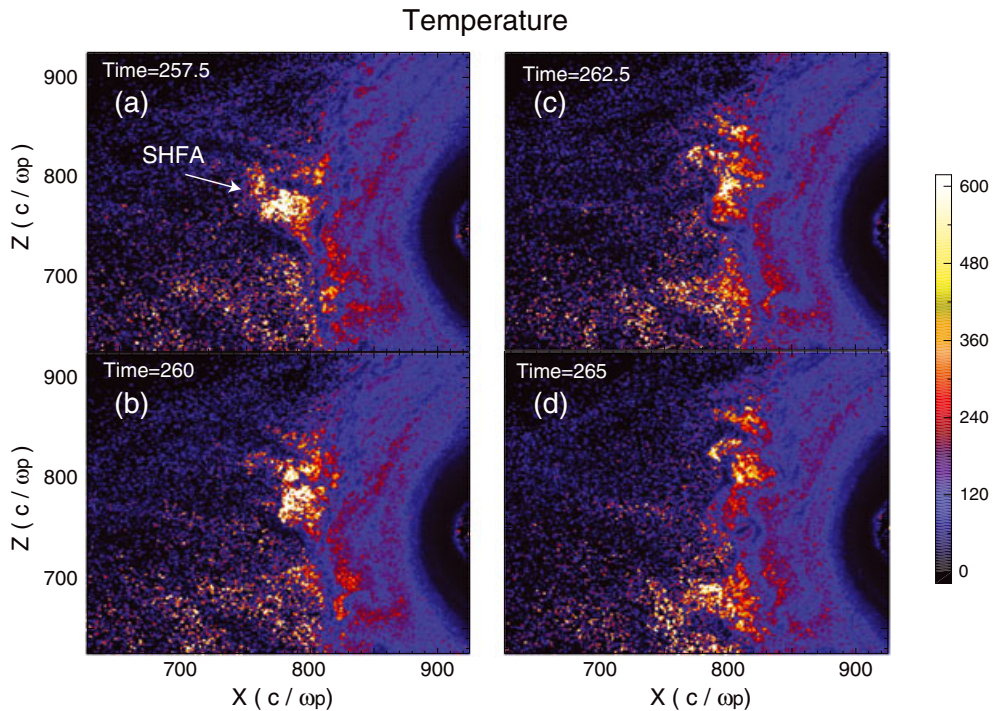


Figure 3. Ion temperature normalized to solar wind value at four times demonstrating injection of energetic ions into the magnetosheath by SHFA.

calculating the second moment of the velocity distribution function and includes the effects of the energetic ions in the foreshock. Figure 2a shows a structure at and upstream of the bow shock consisting of density enhancements surrounding a low density region. An examination of Figure 3a shows that the ion temperature in the low density region is over 600 times hotter than the pristine solar wind. Note that the ion temperature scale in Figure 3 is set to a maximum of 600 for better clarity. This structure looks similar to a simulated HFAs formed at the bow shock due to solar wind discontinuities [e.g., *Omidi and Sibeck, 2007*]. Figures 2b–2d and 3b–3d show the time evolution of this structure that penetrates further

into the magnetosheath and eventually becomes a part of the highly nonuniform and turbulent magnetosheath. In the process the energetic ions within the structure are injected into the magnetosheath.

[9] To see the signature of this structure and its time evolution as might be observed in spacecraft data, Figure 4 shows the ion density, total pressure (normalized to solar wind value), velocity (normalized to V_A) and temperature, as well as the magnetic field (normalized to solar wind value) as observed in time at the location marked by “X” in Figure 2a. As can be seen, the signature consists of enhancements in density and magnetic field (beginning at time $\sim 250 \Omega^{-1}$) that

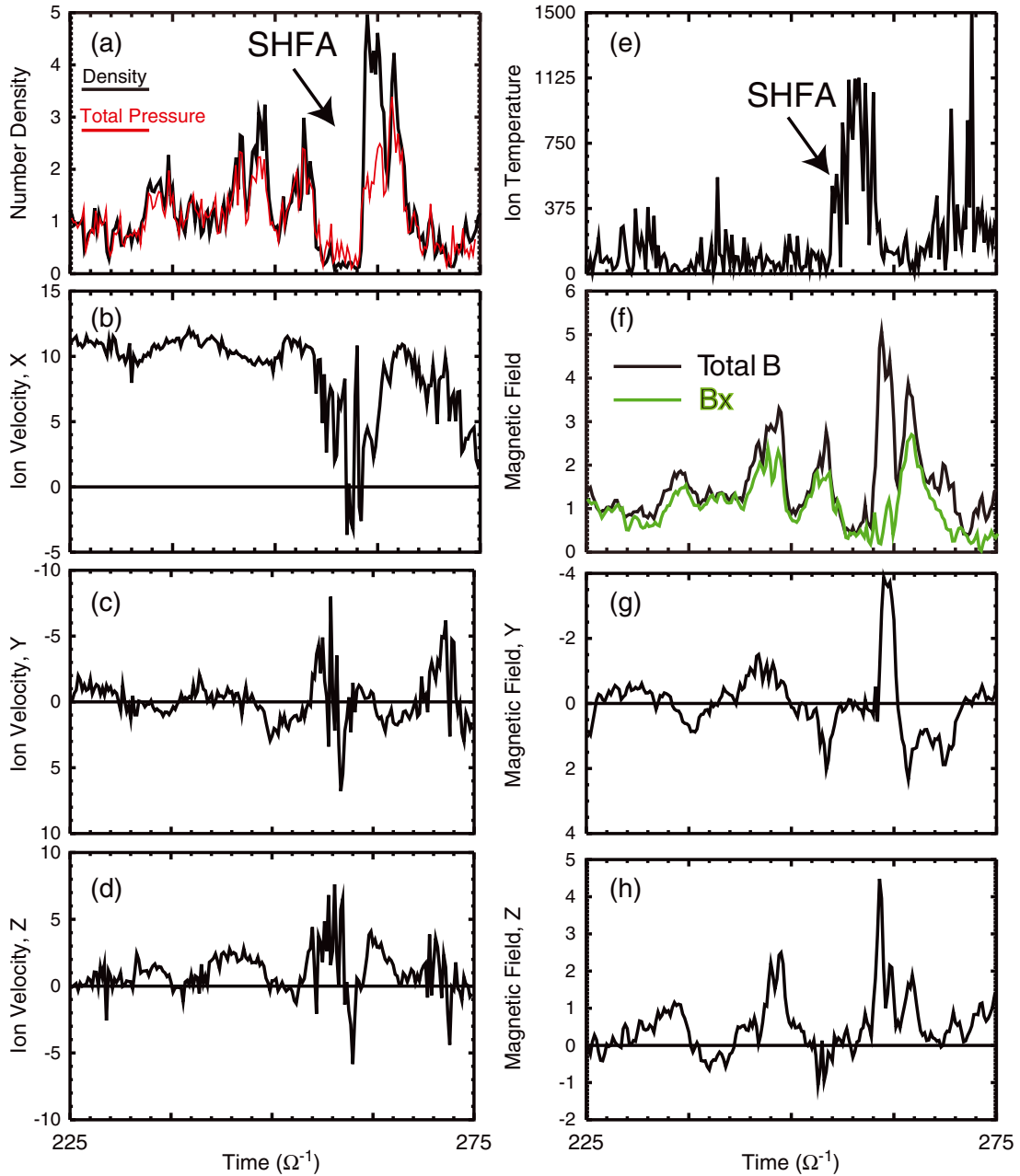


Figure 4. Time series data showing plasma density, three components of velocity, and magnetic field and ion temperature generated at the point marked by “X” in Figure 2a. Density, total pressure, magnetic field, and temperature are normalized to solar wind values and velocities are normalized to the Alfvén speed in the solar wind. The data show signatures of an SHFA.

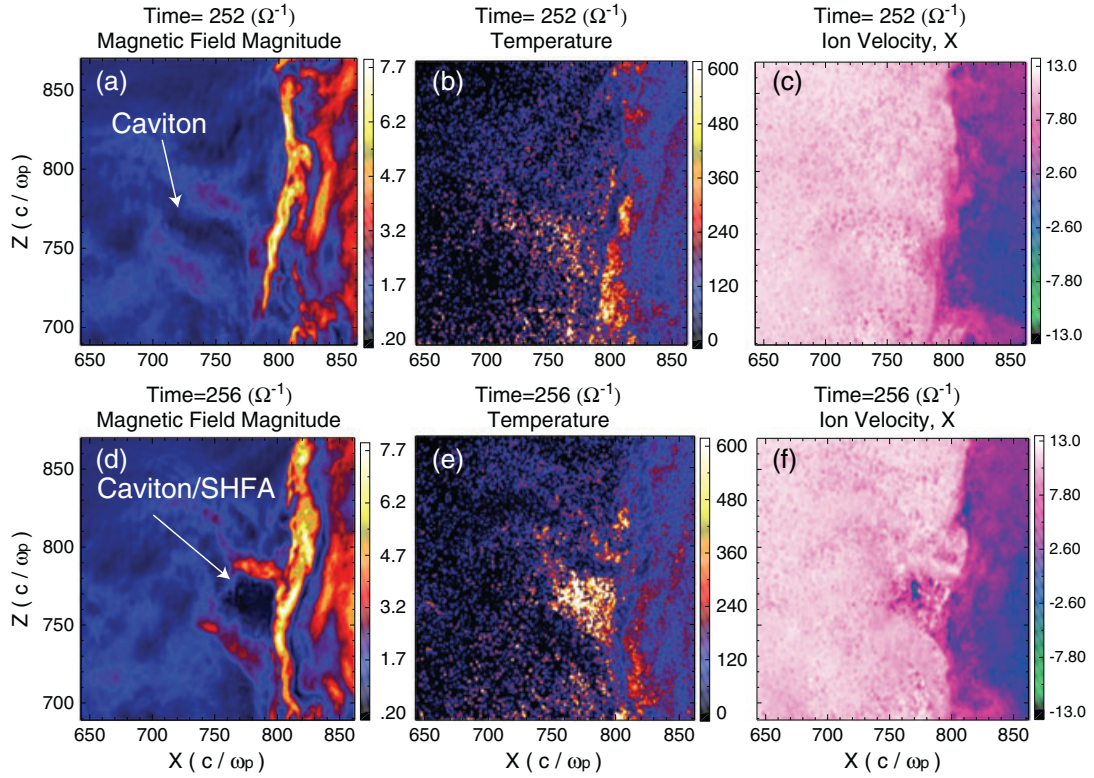


Figure 5. Total magnetic field, ion temperature, and velocity in X direction are shown at two times demonstrating the transformation of a foreshock caviton into a SHFA.

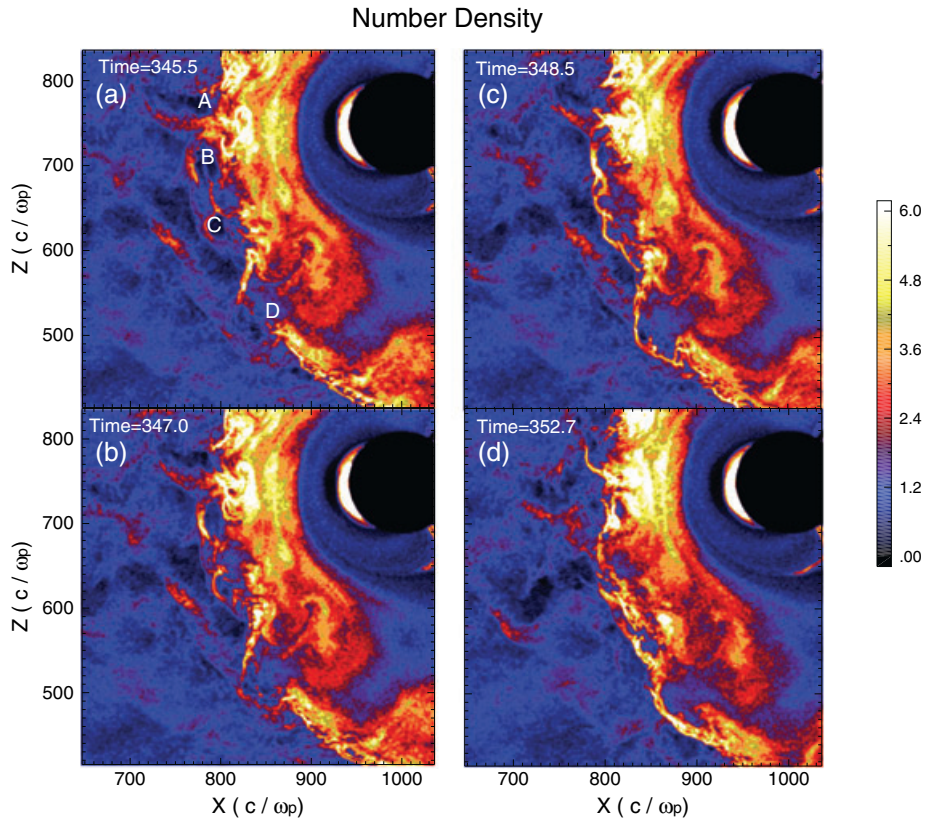


Figure 6. Plasma density at four times showing the evolution of a number of SHFAs as they interact with the bow shock and eventually end up in the magnetosheath.

reach a factor of ~ 3 above the solar wind levels. This is followed by large drops in density (minimum value of $\sim 15\%$ of solar wind density) and field (minimum value of $\sim 30\%$ of solar wind magnetic field) in association with flow deceleration and deflection and enhancements in ion temperature. Note that despite the temperature enhancements, the total pressure in the low density core region is below that in the solar wind. Subsequently, the density and magnetic field increase above the solar wind levels by a factor of ~ 5 before returning to solar wind values. This signature is identical to that of HFAs in general and the SHFAs reported by *Zhang*

et al. (*Zhang, H., et al.*, Spontaneous hot flow anomalies at quasi-parallel shocks: 1. Observations, submitted to *Journal of Geophysical Research*, 2012). Given the absence of a solar wind discontinuity in the simulation, we identify this structure as an SHFA.

[10] To illustrate the formation of this SHFA, Figure 5 shows the total magnetic field, ion temperature, and ion velocity in the X direction at two separate times. Figures 5a–5c show a well-developed foreshock caviton upstream of the bow shock. Figures 5d–5f show that the convection of this caviton by the solar wind into the bow shock transforms it into an SHFA.

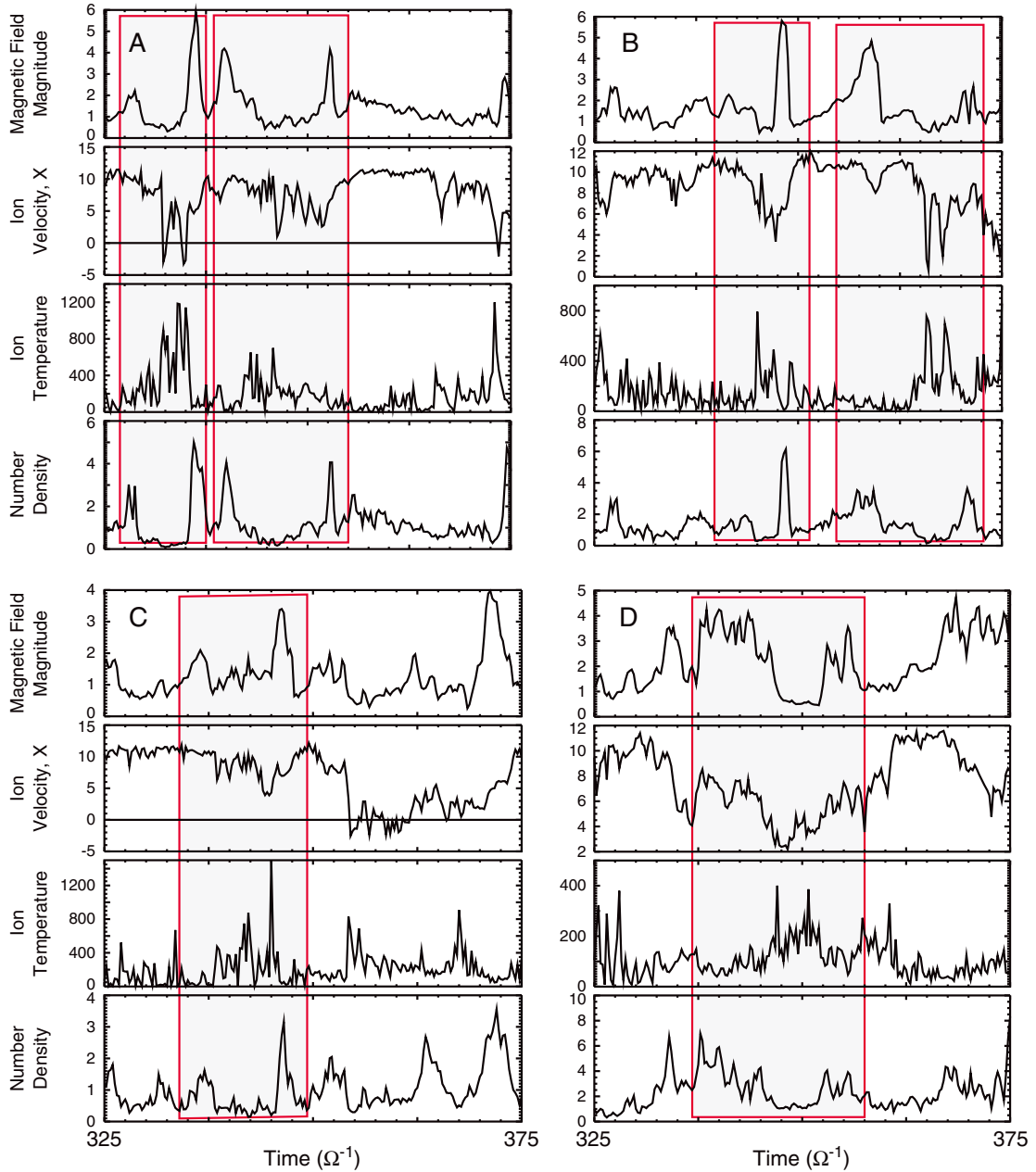


Figure 7. Time series data showing the variations of total magnetic field, flow speed along X , ion temperature, and density at points A, B, C, and D marked in Figure 6a. Density, magnetic field, and temperature are normalized to solar wind values and flow speed is normalized to the Alfvén speed in the solar wind.

This transformation is associated with further energization of the ions in the core of the caviton and the enhancement of the cavity (reduction in magnetic field and density), which in turn increases the magnetic field and density in the outer parts. The details of the ion velocity distribution functions within the SHFA and their time evolution and their relationship to particle energization process remain to be understood and are under investigation. Preliminary results suggest that ion trapping by the cavitons and also ion reflection between the bow shock and the cavitons may play an important role in the acceleration process. Given the convection of the cavitons toward the bow shock, the back and forth motion of ions between the cavitons and the bow shock can result in particle acceleration through first-order and second-order Fermi processes.

[11] Examination of the simulation results show that SHFAs form regularly along the quasi-parallel bow shock surface as isolated foreshock cavitons, such as that in Figure 5, encounter the shock. We also find that at times, multiple cavitons arrive at the bow shock near simultaneously and result in the formation of larger and more complex structures. An example of this is illustrated in Figure 6 that shows the density zoomed around the quasi-parallel shock at four different times. Figure 6a shows the presence of a number of SHFA-like structures along the bow shock that formed at about the same time due to the arrival of multiple foreshock cavitons at the shock. Figures 6b–6d show the time evolution of these SHFAs as they penetrate into the magnetosheath and result in large inhomogeneities and turbulence in the quasi-parallel magnetosheath.

[12] Figure 7 shows the signature of this event in time series data as observed at points “A”, “B”, “C”, and “D” shown in Figure 6a. Density, magnetic field, and temperature are normalized to solar wind values and flow speed is normalized to the Alfvén speed in the solar wind. The data look quite different at each observing point. At point “A”, the data show signatures associated with 2 SHFAs that are shaded. At point “B” two shaded signatures are present that show density and field enhancements and depletions, flow deceleration and the presence of energetic ions, and look similar to SHFAs; however, some differences to SHFAs can also be observed. Similarly, at points “C” and “D” signatures similar to SHFAs are present (shaded regions), but clean and full signatures of SHFAs are harder to identify. In effect the presence of multiple SHFAs at the bow shock and their mutual interactions result in highly nonlinear and complex structures whose signatures in spacecraft data would be similarly complex and hard to decipher.

4. Summary and Conclusions

[13] Motivated by the multispacecraft THEMIS observations of spontaneous hot flow anomalies at the quasi-parallel bow shock by Zhang *et al.* (Zhang, H., *et al.*, Spontaneous hot flow anomalies at quasi-parallel shocks: 1. Observations, submitted to *Journal of Geophysical Research*, 2012), we have examined the structure of a supercritical quasi-parallel bow shock using global hybrid simulations. The results show the formation of copious structures at the quasi-parallel shock whose time series data resemble those of HFAs and SHFAs. Given the steady nature of the solar wind and the absence of a discontinuity in the simulation, these structures are identified as SHFAs. The

formation of SHFAs in the simulation is tied to the convection of foreshock cavitons by the solar wind and their interaction with the bow shock. Foreshock cavitons are structures of the order of $\sim 1 R_E$ (Blanco-Cano *et al.*, 2009, 2011; Kajdič *et al.*, 2010, 2011) consisting of low density and magnetic field core region populated with energetic ions and an outer layer with increased density and magnetic field strength. Transformation of a caviton to an SHFA is associated with further energization of ions, reductions in density and magnetic field in the core of the cavitons, and the enhancements of the density and magnetic field in the outer region. The size of SHFAs in the Z direction is ~ 50 ion skin depths, which is comparable to that of foreshock cavitons and is of the order of $1 R_E$, which is also comparable to the size of HFAs at the bow shock.

[14] Foreshock cavitons have been observed under a wide range of solar wind velocities (Mach number) and IMF orientations. During small and intermediate IMF cone angles when the foreshock falls upstream of the dayside magnetosphere, foreshock cavitons are carried by the solar wind into the bow shock. As a result, we expect the formation of SHFAs at the quasi-parallel bow shock over a wide range of solar wind conditions. Although the simulation results shown here correspond to Alfvén Mach number of 12 and IMF cone angle of 10° , examination of other runs with lower Mach numbers (down to $6 V_A$) and cone angles (smaller than 45°) also shows the formation of SHFAs at the shock. As such, we believe the formation of SHFAs at the quasi-parallel bow shock is a common process and quite significant for ion acceleration and dissipation at the supercritical quasi-parallel bow shock. Similarly, the formation and dissipation of SHFAs as they interact with the bow shock, is critical for determining the properties of the magnetosheath plasma.

[15] The simulation results also demonstrate that when a number of foreshock cavitons arrive and interact with the bow shock near simultaneously, structures larger and more complex than SHFAs are formed. These structures are influenced by the interaction of the cavitons with the bow shock but also with each other. As a result, the time series data obtained at various points along the bow shock are more complex and varied from point to point and exhibit full or partial signatures of multiple SHFAs. Such interactions also lead to large inhomogeneities in the magnetosheath. The results presented by Zhang *et al.* (Zhang, H., *et al.*, Spontaneous hot flow anomalies at quasi-parallel shocks: 1. Observations, submitted to *Journal of Geophysical Research*, 2012) and here demonstrate that ion dissipation processes at the quasi-parallel shock are even more complex than previously thought. Future data analysis and simulations are needed to shine more light on the impacts of SHFAs on the bow shock, magnetosheath, and the magnetosphere. Similarly, differences between HFAs and SHFAs and their magnetospheric impacts need to be explored further. The fact that the formation of HFAs is associated with the presence of solar wind discontinuities while SHFAs form due to the interaction of cavitons with the bow shock provide a means of distinguishing between HFAs and SHFAs. For example, Zhang *et al.* (Zhang, H., *et al.*, Spontaneous hot flow anomalies at quasi-parallel shocks: 1. Observations, submitted to *Journal of Geophysical Research*, 2012) used the absence of a solar wind discontinuity associated with an event to identify it as an SHFA. As we learn more about SHFAs and how they compare and contrast to HFAs, other means of distinguishing between the two may become available.

[16] **Acknowledgments.** Work for this project was supported by NSF grants AGS-1007449, AGS-0963111 and AGS-0962815.

References

- Asbridge, J. R., S. J. Bame, and I. B. Strong (1968), Outward flow of protons from the earth's bow shock, *J. Geophys. Res.*, *73*, 5777, doi:10.1029/JA073i017p05777.
- Blanco-Cano, X., N. Omidi and C. T. Russell (2006a), Macro-Structure of Collisionless Bow Shocks: 2. ULF waves in the foreshock and magnetosheath, *J. Geophys. Res.*, *111*, A10205, doi:10.1029/2005JA01142.
- Blanco-Cano, X., N. Omidi, and C. T. Russell (2006b), ULF waves and their influence on bow shock and magnetosheath structures, *Adv Space Res.*, *37*, 1522, doi:10.1016/j.asr.2005.10.043.
- Blanco-Cano, X., N. Omidi and C. T. Russell (2009), Global hybrid simulations: Foreshock waves and cavitons under radial interplanetary magnetic field geometry, *J. Geophys. Res.*, *114*, A01216, doi:10.1029/2008JA013406.
- Blanco-Cano, X., P. Kajdič, N. Omidi, and C. T. Russell (2011), Foreshock cavitons for different interplanetary magnetic field geometries: Simulations and observations, *J. Geophys. Res.*, *116*, A09101, doi:10.1029/2010JA016413.
- Bonifazi, C., A. Egidi, G. Moreno, and S. Orsini (1980a), Backstreaming ions outside the earth's bow shock and their interaction with the solar wind, *J. Geophys. Res.*, *85*, 3461, doi:10.1029/JA085iA07p03461.
- Bonifazi, C., G. Moreno, A. J. Lazarus, and J. D. Sullivan (1980b), Deceleration of the solar wind in the earth's foreshock region: ISEE 2 and IMP 8 observations, *J. Geophys. Res.*, *85*, 6031, doi:10.1029/JA085iA11p06031.
- Burgess, D. (1989), On the effect of a tangential discontinuity on ions specularly reflected at an oblique shock, *J. Geophys. Res.*, *94*, 472, doi:10.1029/JA094iA01p00472.
- Eastwood, J. P., et al. (2008), Themis observations of a hot flow anomaly: Solar wind, magnetosheath, and ground-based measurements, *Geophys. Res. Lett.*, *35*, 332, doi:10.1029/2008GL033475.
- Facsko, G., et al. (2008), A statistical study of hot flow anomalies using Cluster data, *Adv Space Res.*, *41*(8), 1286, doi:10.1016/j.asr.2008.02.005.
- Gosling J. T., J. R. Asbridge, S. J. Bame, G. Paschmann, and N. Scopke (1978), Observations of two distinct populations of bow shock ions in the upstream solar wind, *J. Geophys. Res.*, *5*, 957, doi:10.1029/GL005i01p00957.
- Greenstadt, E. W., et al. (1968), Correlated magnetic field and plasma observations of the Earth's bow shock, *J. Geophys. Res.*, *73*, 51, doi:10.1029/JA073i001p00051.
- Greenstadt, E. W., C. T. Russell, V. Formisano, et al. (1977), Structure of a quasi-parallel, quasi-laminar bow shock, *J. Geophys. Res.*, *82*, 651, doi:10.1029/JA082i004p00651.
- Greenstadt, E. W., C. T. Russell, and M. Hoppe (1980), Magnetic field orientation and suprathermal ion streams in the earth's foreshock, *J. Geophys. Res.*, *85*, 3473, doi:10.1029/JA085iA07p03473.
- Greenstadt, E. W., et al. (1993), The quasiperpendicular environment of large magnetic pulses in Earth's quasi-parallel foreshock: ISEE 1 & 2 observations, *Geophys. Res. Lett.*, *20*, 1459, doi:10.1029/93GL00841.
- Greenstadt, E. W., et al. (1995), ULF waves in the foreshock, in *Physics of Collisionless Shocks*, ed. C. T. Russell, *Adv Space Res.*, Pergamon, 71.
- Jacobsen, K. S., et al. (2009), THEMIS observations of extreme magnetopause motion caused by a hot flow anomaly, *J. Geophys. Res.*, *114*, doi:10.1029/2008JA013873.
- Kajdič, P., X. Blanco-Cano, N. Omidi, and C. T. Russell (2010), Analysis of waves surrounding the foreshock cavitons, *AIP Conf. Proc.*, *1216*, 479, doi:10.1063/1.3395907.
- Kajdič, P., X. Blanco-Cano, N. Omidi, and C. T. Russell (2011), Multi-spacecraft study of foreshock cavitons upstream of the quasi-parallel Earth's bow shock, *Planet. Space Sci.*, *59*, 705, doi:10.1016/j.pss.2011.02.005.
- Le, G. and C. T. Russell (1992), A study of ULF wave foreshock morphology, II: Spatial variations of ULF waves, *Planet. Space Sci.*, *40*.
- Lin, Y. (1997), Generation of anomalous flows near the bow shock by its interaction with interplanetary discontinuities, *J. Geophys. Res.*, *102*, 24265.
- Lin, Y. (2002), Global hybrid simulation of hot flow anomalies near the bow shock and in the magnetosheath, *Planet. Space Sci.*, *50*, 577, 2002.
- Lin Y. (2003), Global-scale simulation of foreshock structures at the quasi-parallel bow shock, *J. Geophys. Res.*, *108*, 1390, doi:10.1029/2003JA009991.
- Lin, Y., and X. Wang (2005), Three-dimensional global hybrid simulation of dayside dynamics associated with the quasiparallel bow shock, *J. Geophys. Res.*, *110*, A12216, doi:10.1029/2005JA011243.
- Lucek, E. A., et al. (2004), Cluster observations of hot flow anomalies, *J. Geophys. Res.*, *109*, A06207, doi:10.1029/2003JA010016.
- Omidi, N. (2007), Formation of cavities in the foreshock, in *Turbulence and Nonlinear Processes in Astrophysical Plasmas*, edited by D. Shaikh and G. Zank, *AIP Conference Proceedings*, *932*, 181.
- Omidi, N. and D. G. Sibeck (2007), Formation of hot flow anomalies and solitary shocks, *J. Geophys. Res.*, *112*, A01203, doi:10.1029/2006JA011663.
- Omidi, N., K. B. Quest, and D. Winske (1990), Low mach number parallel and quasi-parallel shocks, *J. Geophys. Res.*, *95*, 20,717–20,730.
- Omidi, N., X. Blanco-Cano, C. T. Russell, and H. Karimabadi (2004), Dipolar magnetospheres and their characterization as a function of magnetic moment, *Adv. Space Res.*, *33*(11), 1996.
- Omidi, N., X. Blanco-Cano and C. T. Russell (2005), Macro-structure of collisionless bow shocks: 1. Scale lengths, *J. Geophys. Res.*, *110*, A12212, doi:10.1029/2005JA011169.
- Omidi, N., X. Blanco-Cano, C. T. Russell and H. Karimabadi (2006), Global hybrid simulations of solar wind interaction with Mercury: Magnetospheric boundaries, *Adv. Space Res.*, doi:10.1016/j.asr.2005.11.019.
- Omidi, N., T. Phan, and D. G. Sibeck (2009a), Hybrid simulations of magnetic reconnection initiated in the magnetosheath, *J. Geophys. Res.*, *114*, A02222, doi:10.1029/2008JA013647.
- Omidi, N., D. Sibeck and X. Blanco-Cano (2009b), Foreshock compressional boundary, *J. Geophys. Res.*, *114*, A08205, doi:10.1029/2008JA013950.
- Omidi, N., J. P. Eastwood, and D. G. Sibeck (2010), Foreshock bubbles and their global magnetospheric impacts, *J. Geophys. Res.*, *115*, A06204.
- Paschmann, G., et al. (1979), Association of low frequency waves with suprathermal ions in the upstream solar wind, *Geophys. Res. Lett.*, *6*, 209.
- Paschmann, G., et al. (1988), 3-Dimensional plasma structures with anomalous flow directions near the Earth's bow shock, *J. Geophys. Res.*, *93*, 11279.
- Russell, C. T. and M. Hoppe (1983), Upstream waves and particles, *Space Sci Revs*, *34*, 155.
- Russell, C. T. (1988), Multipoint measurements of upstream waves, *Adv. Space Res.*, *8*, 147.
- Scholer, M., M. Fujimoto and H. Kucharek (1993), 2-dimensional simulations of supercritical quasi-parallel shocks- upstream waves, downstream waves and shock re-formation, *J. Geophys. Res.*, *98*, 18971.
- Schwartz, S. J., et al. (1988), Active current sheets near the earth's bow shock, *J. Geophys. Res.*, *93*, 11295.
- Schwartz, S. J. (1995), Hot flow anomalies near the earth's bow shock, in *Physics of Collisionless Shocks*, edited by C. T. Russell, 107 p., *Advances in Space Research*, Pergamon.
- Schwartz, S. J., et al. (2000), Conditions for the formation of hot flow anomalies, *J. Geophys. Res.*, *105*, 12639.
- Sibeck, D. G., et al. (1998), Gross deformation of the dayside magnetopause, *Geophys. Res. Lett.*, *25*(4), 453.
- Sibeck, D. G., et al. (1999), Comprehensive study of the magnetospheric response to a hot flow anomaly, *J. Geophys. Res.*, *104*, 4577.
- Sibeck, D. G., et al. (2000), Magnetopause motion driven by interplanetary magnetic field variations, *J. Geophys. Res.*, *105*, 25,155.
- Sibeck, D. G., N. Omidi, I. Dandouras, and E. Lucek (2008), On the edge of the foreshock: model-data comparisons, *Ann. Geophys.*, *26*, 1539.
- Thomas, V. A., D. Winske and N. Omidi (1990), Reforming super-critical quasi-parallel shocks, 1. One- and two-dimensional simulations, *J. Geophys. Res.*, *95*, 18809.
- Thomas, V. A., D. Winske, M. F. Thomsen and T. G. Onsager (1991), Hybrid simulation of the formation of a hot flow anomaly, *J. Geophys. Res.*, *96*, 11625.
- Thomsen, M. F., et al. (1986), Hot diamagnetic cavities upstream from the earth's bow shock, *J. Geophys. Res.*, *91*, 2961.
- Thomsen, M. F., et al. (1988), On the origin of hot diamagnetic cavities near the earth's bow shock, *J. Geophys. Res.*, *93*, 11311.
- Thomsen, M. F., et al. (1990a), Two-state ion heating at quasi-parallel shock, *J. Geophys. Res.*, *95*, 957.
- Thomsen, M. F., J. T. Gosling, S. J. Bame, and C. T. Russell (1990b), Magnetic pulsations at the quasi-parallel shock, *J. Geophys. Res.*, *95*, 957.
- Thomsen, M. F., et al. (1993), Observational test of hot flow anomaly formation by the interaction of a magnetic discontinuity with the bow shock, *J. Geophys. Res.*, *98*, 15319.
- Winske, D., N. Omidi, K. B. Quest, and V. A. Thomas (1990), Reforming supercritical quasi-parallel shocks: 2. Mechanism for wave generation and front reformation, *J. Geophys. Res.*, *95*, 18,821.
- Winske, D. and N. Omidi (1993), Hybrid codes: Methods and applications, in *Computer Space Plasma Physics: Simulation Techniques and Software*, edited by H. Matsumoto, and Y. Omura, 103 p., Terra Scientific.
- Winske, D., and N. Omidi (1996), A nonspecialist's guide to kinetic simulations of space plasmas, *J. Geophys. Res.*, *101*, 17287.